DYNAMICS OF ULTRALOW-q PLASMAS IN THE RFX-MOD DEVICE

M. Zuin[1], M. Agostini[1], F. Auriemma[1], D. Bonfiglio[1], S. Cappello[1], L. Carraro[1], R. Cavazzana[1], L. Cordaro[1], P. Franz[1], L. Marrelli[1], E. Martines[1,2], M.E. Puiatti[1], R. Piovan[1], G. Spizzo[1], D. Terranova[1], N. Vianello[1], P. Zanca[1], B. Zaniol[1], L. Zanotto[1]
[1] *Consorzio RFX, Corso Stati Uniti 4, 35127 Padova, Italy*
[2] *Dipartimento di Fisica 'Giuseppe Occhialini', Universitá degli Studi di Milano - Bicocca, Piazza della Scienza 3, 20126 Milano, Italy*
(Dated: November 26, 2021)

The results are presented of an experimental activity performed in the RFX-mod device aimed at characterizing plasma dynamics in the so-called ultralow-q (ULq) magnetic configuration, which corresponds to edge safety factor values below 1. The role of the edge safety factor in determining plasma dynamics is studied. In particular, a characterization of MHD activity is performed.

The results of dedicated non-linear 3D visco-resistive MHD simulations are in good quantitative agreement with the experimental observations. In particular, the predicted tendency for ULq plasmas to be characterized by magnetic spectra dominated by a single mode (either a kink or a double resonant internal mode) is confirmed by experiment.

Magnetic reconnection plays a relevant role in determining the dynamics of the magnetic topology. Both almost quiescent and largely fluctuating plasmas are observed with a strong sensitivity on the edge safety factor. The main MHD properties of the ULq are compared to those of RFP and tokamak discharges, also produced in the RFX-mod device.

MHD modes exhibit toroidal rotation at a frequency depending on mode amplitude. Differently from what encountered in RFP plasmas at comparable current levels, no wall locking is detected.

I. INTRODUCTION

The confinement of hot plasmas for fusion in toroidal devices relies on a combination of magnetic fields, which can be supplied by external coils and/or produced by an induced plasma current, i.e. exploiting the self-confining pinch effect [1].

In magnetohydrodynamic (MHD) theory, the equilibrium and linear stability of a configuration are conveniently characterized in terms of the safety factor q, which gives the magnetic field line pitch as a function of plasma minor radius (in cylindrical approximation $q(r) = rB_z/RB_\theta$, being r the radial coordinate and R the plasma major radius, B_z and B_θ the axial and azimuthal magnetic field components, respectively). Its value gives a measure of the relevance of the magnetic field produced by currents flowing in external coils (external coils are mostly responsible for B_z) with respect to that of B_θ, self-produced by the plasma current.

Devices which heavily rely on plasma current have low q values. The various magnetic configurations can thus be characterized by the common parameter $q(a)$, where a is the minor radius of the torus at the plasma boundary (general considerations about the classification of different confinement concepts are summarized, for example, in figure 24, p 1042 of [2], or in [3], see the introductory chapter 1, section 1.5).

In tokamaks, $q(a)$ is always positive and greater than unity. Normal tokamak discharges have $q(a) > 3$. Discharges with $1 < q(a) < 2$ are referred to as low-q (Lq) tokamak discharges. Reversed-field pinch (RFP) discharges have negative $q(a)$ values because of the field reversal. In-between the Lq tokamak and the RFP stands the Ultra low-q (ULq) configuration, corresponding to $0 < q(a) < 1$. The term ULq includes a class of equilibria with largely different MHD stability properties and behaviour. It is worth to notice that ULq states can transitorily exist in the RFP setup phase, when the plasma current rises, but $q(a)$ is still above zero.

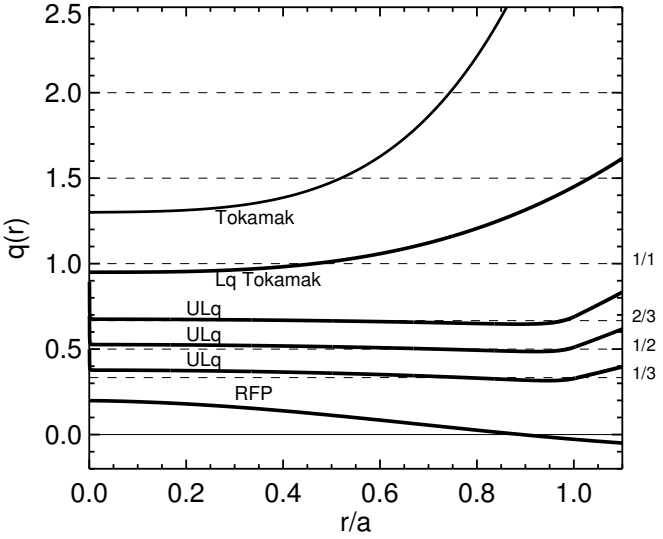

FIG. 1: Examples of radial safety factor profiles, $q(r)$, for various magnetic configurations: Tokamak, Low-q Tokamak (Lq Tokamak), Ultralow-q (ULq) and Reversed-field pinch (RFP).

The first dedicated studies of the ULq regimes were reported already at the very beginning of the research on thermonuclear fusion (references can be found in [4]). In the late 50s stabilized pinch discharges were

implemented and studied in ZETA [5]. Later on, the linear ideal MHD stability analysis by Robinson [6] had very early on pointed out that ULq equilibrium can be linearly unstable with respect to both external and internal modes. In particular, a pitch minimum can lead to both pressure driven and current driven instabilities. It was shown that current driven double resonant surface (DRS) modes (i.e. modes whose resonance is present in two distinct radial positions within the plasma) with $m = 1$ are ideally unstable when a corresponding resonant surface is inside the plasma [6], [7]; $m = 2$ double resonant modes could also become unstable, but with smaller growth rates [7]. A substantial increase of the $m = 2$ modes growth rate is, however, expected to be induced by the destabilizing effect of finite $\beta = \frac{2\mu_0 p}{B^2}$, the parameter relating the plasma kinetic pressure, p, to the one exerted by the confining magnetic field, $\frac{B^2}{2\mu_0}$. Such theoretical considerations induced a significant reduction of studies in this area. A renewed interest grew up in connection with the MHD relaxation phenomena [8, 9] and dedicated ULq studies were experimentally performed in various devices including Toriut-6 [10], Repute-1 [11], HBTX-1C [12] and OHTE [14].

Despite the high attained β values, the estimated energy confinement time, which measures the rate of energy loss (ratio between the plasma energy content in a steady state and the power needed to sustain it) has been found to be pretty low [2, 3, 10].

Nevertheless, some basic aspects in low q configurations are still attractive, notably:

- the relatively low magnetic field to be supplied by the external coils,
- the efficiency of plasma heating by ohmic dissipation of the plasma current,
- the observed possibility of overcoming the Greenwald limt with no disruption or radiative collapse [13, 40],
- the observation of ion temperatures similar to or even larger than the electron temperatures [11].

It is important to note that ULq plasmas could also give interesting contributions to the physics of tokamak plasmas, where direct and effective measurements of core MHD behaviors and magnetic fluctuations are difficult. The ULq profiles are similar to those of the core region of tokamak plasmas, so that ULq studies could contribute to the understanding about the underlying physical mechanisms and developing operation/control techniques for tokamak plasmas.

Moreover, with the aim of proposing ways to improve the confinement properties, active modification of dynamo activity and self-organization processes has been investigated in both ULq and RFP by means of pulsed poloidal and toroidal electric fields [15–17, 46, 47]. Synchronized to the application of the pulsed electric fields, a remarkable response of the several ULq plasma parameters had been observed. The plasma showed a preferential magnetic field structure, and the external perturbation activates fluctuation to maintain the structure through dynamo effect. This process changes the total dissipation with the variation of magnetic helicity in the system, showing that self-organization accompanies an enhanced dissipation. Transient reduction of plasma-wall interaction during dynamic magnetic compression has also been reported in the REPUTE-1 ULq plasmas [15].

From a topological point of view, along with different $q(a)$ values, the various magnetic configurations (tokamak, ULq and RFP) exhibit $q(r)$ profiles with different features. In particular, while standard tokamaks normally have $\frac{dq}{dr} > 0$, ULq and RFP configurations are described by $\frac{dq}{dr} < 0$ profile in the plasma core (indeed, decreasing $q(r)$ profiles were found in TORIUT-6 and increasing in OHTE). A schematic representation of possible equilibrium $q(r)$ profiles is shown in Fig.1 for four magnetic configurations (Tokamak, Lq Tokamak, ULq and RFP). The ULq normally exhibits a $q(r)$ minimum at the edge, which is removed in the RFP equilibrium.

As suggested in [10] the differences in the equilibrium profiles should be determined by differences in the dissipative processes which determine the equilibrium profiles. In [18] Tokamaks and RFPs have been proposed as associated with different dissipative branches: the classical resistive diffusion would be mainly responsible for Tokamak dynamics, while MHD resistive-kink activity and the induced relaxation would be at the origin of broad current density profiles in RFPs. The ULq dynamics is interpreted as a competitive process between MHD relaxation and classical diffusion.

The paper is organized as follows: section II is dedicated to a description of the experimental and diagnostic set-up; in section III the various experimental results are presented and compared to modeling predictions. Discussion and conclusion sections follow.

II. EXPERIMENTAL AND DIAGNOSTIC SET-UP

This paper is dedicated to the results of experimental campaigns devoted to the study of ULq plasmas in the RFX-mod device. In particular, three campaigns have been produced in the last years. In the first two of them Hydrogen and in the third Deuterium were used as main working gas. In general, due to the reduced number of shots no direct isotope effects will be hereafter discussed and the database will be considered as homogenous in terms of ion mass.

RFX-mod is a toroidal device ($R = 2$ m, $a = 0.46$ m, R and a major and minor radii, respectively), with circular shape, whose main purpose is the study of the RFP configuration at high plasma current levels (up to 2 MA). It is equipped with a thin conductive wall located at $r_{wall} = 0.51$ m.

One of the main characteristics of the RFX-mod device is its sophisticated real-time feedback system, made of 192 independently fed, saddle coils, fully covering the

machine, whose aim is to mimic a close ideal (thick) shell. This system is made of 4 arrays, equally spaced along the poloidal direction, of 48 saddle coils each, equally spaced along the toroidal direction.

Thanks to such system, the active feedback control of magnetic perturbations with poloidal mode number $m \leq 2$ and toroidal mode number $n \leq 24$ can be performed. Its exploitation made possible during RFP operations to strongly reduce the plasma-wall interaction related to the so-called dynamo modes (internal kink-resistive modes) and to fully control resistive wall modes, RWMs (see [19, 20, 36] and references therein).

The enhanced control capability gave access to improved confinement regimes in high current RFP plasmas, associated with the emergence within the magnetic spectrum of Quasi Single Helical regimes, i.e. the condensation of the perturbation energy in one single mode (and its harmonics). In particular, the spontaneous occurrence of a self-organized helical equilibrium with a single helical axis, reduced magnetic fluctuations and strong transport internal barriers has been reported [21, 22].

RFX-mod can also be operated as a low field (maximum toroidal field is 0.6 T), low plasma current tokamak. Thanks to the RFX-mod feedback system, exploited to actively control the $m/n = 2/1$ external kink, also low-q tokamak conditions have been routinely produced in both circular and shaped (single null and double null) plasmas [23].

The characterization of the MHD activity is based on a system of edge in-vessel coils, which constitute part of the ISIS (Integrated System of Internal Sensors) diagnostic system, measuring the time derivative of the magnetic field fluctuations (through flux variation)[24]. The probes are located behind the graphite tiles of the first wall in various toroidal and poloidal positions. In particular, part of these probes, measuring the toroidal magnetic field fluctuations, are distributed on two toroidal arrays, each made of 48 equally spaced coils, in two poloidal positions (at $\theta = 70°$ and $\theta = 250°$, being $\theta = 0°$ on the low-field equatorial plane and positive $\theta > 0$ pointing upwards). A poloidal array of 8 equally spaced probes along the poloidal direction measures the time derivative of the toroidal magnetic field at a given toroidal position, and two similar arrays measure the time derivative of the radial and poloidal magnetic field components. Sampling frequency is 2 MHz, the estimated bandwidth of the measurements is up to 500 kHz. The arrays allow a resolution of the toroidal and poloidal mode numbers n and m up to 24 and 4, respectively (plasma instabilities are, as usually, represented by Fourier modes in the poloidal and toroidal angles, θ and ϕ, as $e^{i(m\theta - n\phi)}$).

ULq plasmas have been produced with the following set of parameters: plasma current $I_p = 250-800$ kA, loop voltage $V_{loop} = 20-50$ V, $q(a) = 0.2-1$, toroidal field B_ϕ up to 0.5 T, pulse duration ~200 ms and electron density $n_e \sim (1-8) \times 10^{19} m^{-3}$. Considering that ULq plasmas on RFX-mod show an electron temperature in the range 100-300 eV and assuming unitary plasma effective charge Z_{eff} (due to the lack of direct measurement), the upper limit for the estimated Lundquist number S is roughly $S \sim 10^6$.

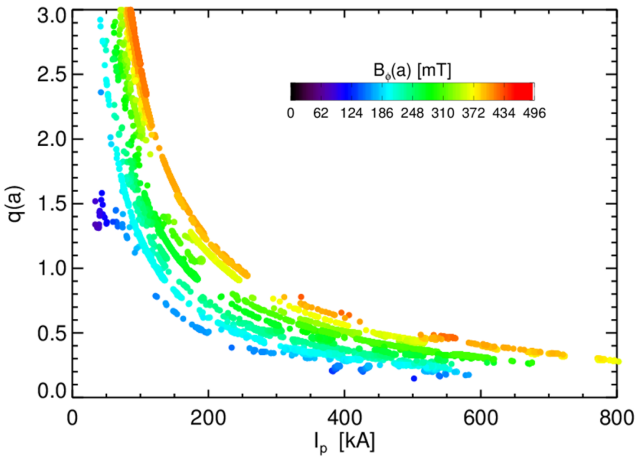

FIG. 2: Considered discharges database including ULq, Lq and tokamak plasmas: edge safety factor $q(a)$ as a function of the plasma current I_p. Colors refer to the various applied edge toroidal magnetic fields. Each point is an average over different flat-top phases within the discharges.

As mentioned, along with ULq discharges the database for the present analysis takes into account RFP and tokamak (circular) discharges produced in RFX-mod for a direct comparison between the various magnetic configurations. In Fig.2 the database referring to ULq, Lq and tokamak discharges is shown in terms of $q(a)$ and I_p, each point representing an average over different flat-top phases of the plasma current, the color scale referring to the toroidal magnetic field at the edge $B_\phi(a)$.

From the operational point of view, discharges are performed by controlling basically the loop voltage and the edge value of the toroidal field $B_\phi(a)$. A uniform toroidal field is initially applied, the plasma current is raised in less than 10 ms to its maximum value (so that a transition from a low-current Tokamak to the ULq configuration occurs) and then kept constant during the flat-top discharge phase. The value of $q(a)$ after the current rise is determined by the plasma current and the initial toroidal field. Few examples of discharges behavior are presented in Fig.3. Discharge optimization is played by density control, realized by careful wall cleaning in between discharges and searching for optimum filling pressure. In this respect, the equilibrium control by vertical field coils also plays a fundamental role by limiting the horizontal shift and plasma-wall interaction.

III. EXPERIMENTAL RESULTS

A. MHD behaviour

In general, similarly to other previous experiments [10, 45], a natural tendency is found to sustain the configurations at discrete q-values at the edge, next to the major rational $q(a)$ values. The extreme sensitivity of ULq discharges to the $q(a)$ value is shown in Fig. 3, where the time traces of some of the main discharge signals (plasma current I_p, toroidal loop voltage V_{loop}, edge toroidal field $B_\phi(a)$ and the corresponding $q(a)$) are shown for four different shots, all with the same applied toroidal field. It is evident, comparing for example shots #23016 and #23025 (green and magenta traces), how a slight change of $q(a)$ in the flat top phase corresponds to significantly different plasma behaviors, the first shot being characterized by large bursty fluctuation on all the quantities shown, more evident on the V_{loop} signal, the latter by a long lasting, more quiet, flat-top phase. To highlight the different behaviour in terms of fluctuation of the various discharges, the rms of the V_{loop} is also shown, evaluated on 5 ms time windows in the flat-top phase.

This dynamics is dominated by MHD instabilities with a wide range of m, n mode numbers. In most cases, a single mode almost dominates the magnetic fluctuation spectrum, whose amplitude can grow and saturate at a given amplitude for a finite time interval, or exhibit sawtoothing-like behavior, with associated relaxation of the $q(r)$ profile, also visible as strong fluctuation of the plasma current. The discontinuous change in q stems from the instability of global kink modes, as already described in [10, 45].

In Fig. 4, an example is given of the variety of possible MHD behavior for the same discharges as in Fig.3. The color-coded contour plots represent the toroidal magnetic fluctuations along the toroidal direction and of the radial field along the poloidal direction, in a 10 ms interval during the flat-top phase. Comparing shots #23016 and #23025, whose dynamics is dominated by the same $m/n = 2/5$ mode with comparable amplitude, it is interesting to observe how the global plasma behavior can be either almost quiescent (#23025) or largely fluctuating (#23016). The activity of such $m/n = 2/5$ mode is reflected in the V_{loop} signal, which can exhibit oscillations up to 30 V, sign of global internal rearrangements of the plasma current profile.

In the last row of Fig.4, the $q(r)$ profile at a central time in the chosen window, $t = 75$ ms, is estimated by means of a classical $\alpha - \theta_0$ model normally adopted to describe RFP equilibrium [25]. In such model, the function $\sigma(r)$, which links the equilibrium (zeroth order) current density J_0 and the equilibrium field B_0 through $\mu_0 J_0 = \sigma(r) B_0$, is parametrized as $\sigma(r) = 2\frac{\theta_0}{a}(1 - r/a)^\alpha$, and α and θ_0 are optimized by using current and external magnetic measurements in a toroidal geometry.

The plasma current evolution generally exhibits a staircase-like behavior, with a natural tendency to sustain the configurations with discrete q values at the edge (a clear example of a discharge with this behavior is shown in Fig.5).

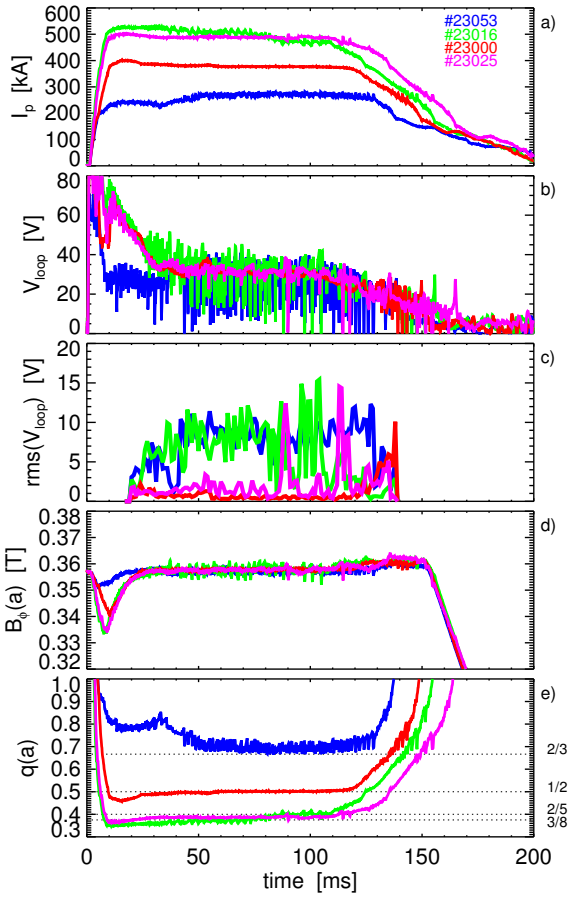

FIG. 3: Time traces of various quantities for four ULq discharges, corresponding to different edge safety factor values (indicated with different colors): a) plasma current, I_p; b) toroidal Ohmic loop voltage, V_{loop}; c) rms of the V_{loop}, evaluated on 5 ms windows in the flat-top phase; d) edge toroidal magnetic field $B_\phi(a)$; e) edge safety factor $q(a)$.

The flat plasma current phases can be associated to both almost quiet conditions or largely fluctuating ones (as can be observed on the V_{loop} signal shown in Fig.5c) and are normally preceded by the growth of very large single modes with m/n depending on the q-value at the edge. A large kink deformation of the plasma column, with strong interaction with the wall, is present during the raise of the mode. An example of the image collected from an internal CCD camera is shown in Fig.6, where a clear helical pattern in the first-wall emission is visible, corresponding to a significant plasma column deformation (due to a $m/n = 1/4$ large dominant mode in the case presented).

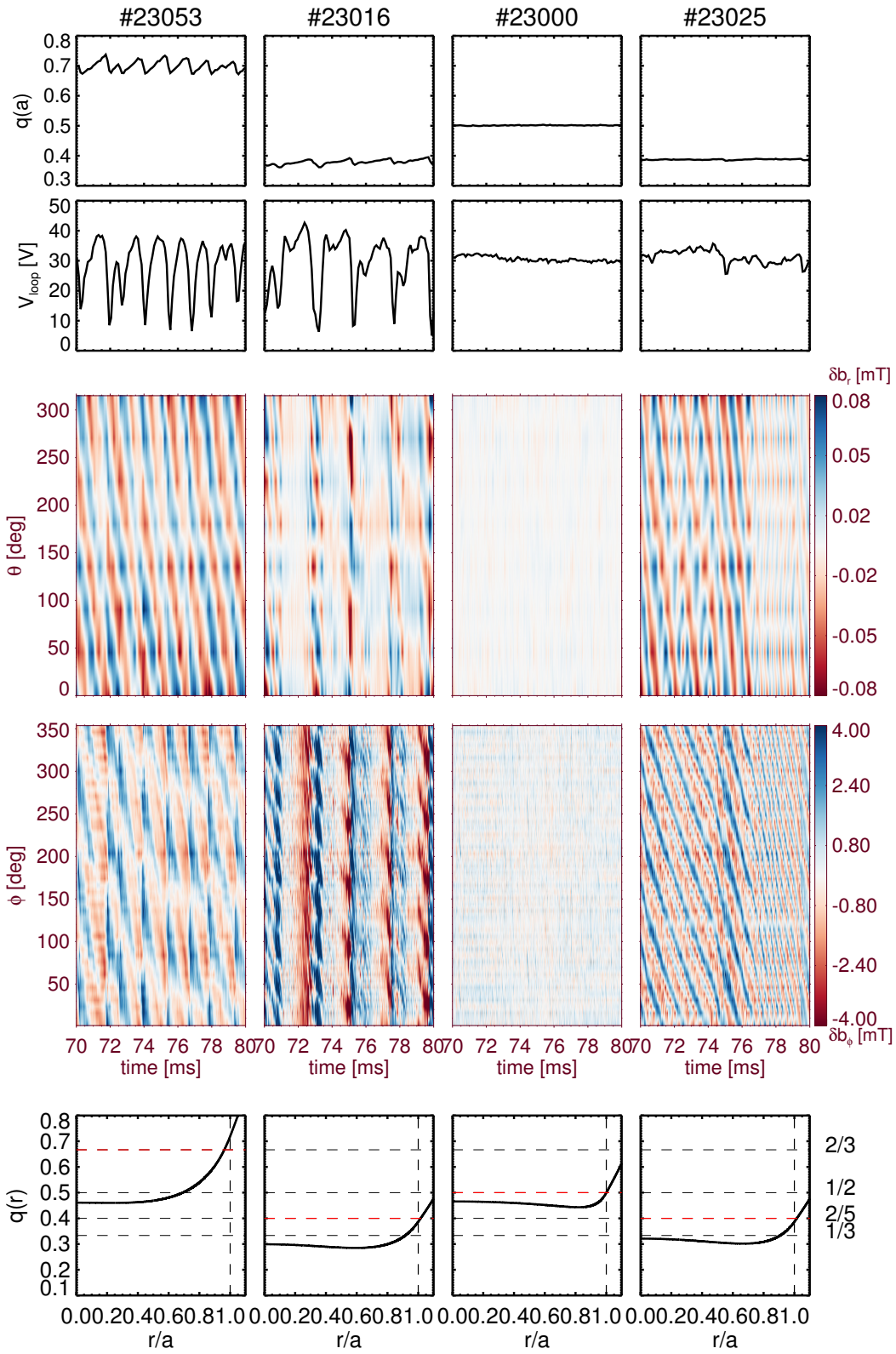

FIG. 4: First row: time evolution of the edge safety factor $q(a)$ in a flat-top phase for the same 4 discharges as in Fig.3. Second row: toroidal loop voltage; third row: contour plot of the radial magnetic field fluctuation along the full poloidal array of 8 probes; fourth row: contour plot of the toroidal magnetic field fluctuation along the full toroidal array of 48 probes; fifth row, reconstruction of the $q(r)$ profile at the time $t = 75$ ms.

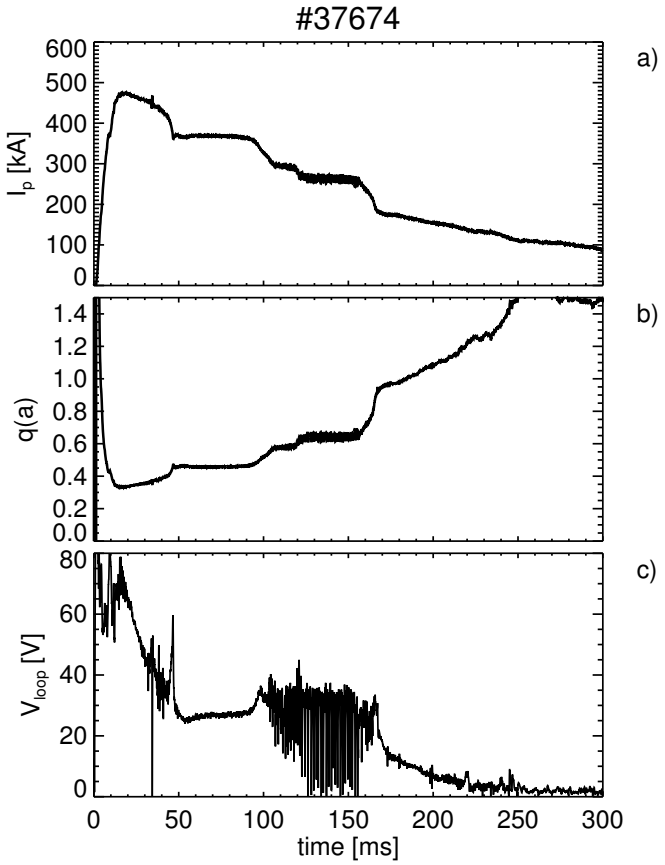

FIG. 5: Time evolution of a discharge which exhibits evident staircase-like behavior of the plasma current, panel a). In panels b) and c) the time traces of $q(a)$ and V_{loop} signals are shown, respectively.

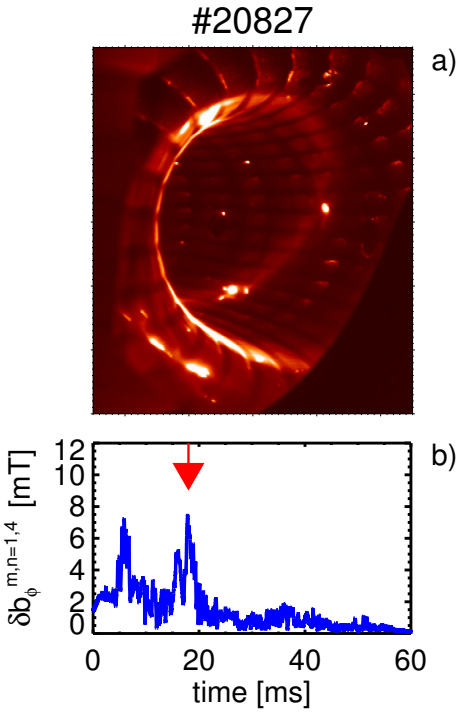

FIG. 6: a) image (false colors) from an internal CCD camera collected at the time instant indicated by a red arrow in panel b. A helical pattern is visible as the sign of an enhanced plasma-wall interaction. b) time evolution of the amplitude (toroidal magnetic field component) of the dominant $m/n = 1/4$ mode, $\delta b_\phi^{m/n=1/4}$.

B. Comparison with MHD simulations

The macroscopic behavior of ULq configurations can be compared to that predicted by a simple visco-resistive MHD zero-β approximation which describes 3D nonlinear dynamics with the numerical code SpeCyl. Here, we briefly remind the basics of this approach (see, for example [26] and references therein or, for more detail about the numerical analysis, reference [27]. The visco-resistive compressible MHD equations in the constant-pressure constant-density approximation including resistivity, η, and viscosity, ν, can be written in dimensionless units as

$$\frac{\partial \mathbf{B}}{\partial t} = \nabla \times (\mathbf{v} \times \mathbf{B} - \eta \mathbf{J}) \qquad (1)$$

$$\rho[\frac{\partial \mathbf{v}}{\partial t} + (\mathbf{v} \cdot \nabla)\mathbf{v}] = \mathbf{J} \times \mathbf{B} + \rho\nu\nabla^2\mathbf{v} \qquad (2)$$

Here, $\mathbf{B}$ is the magnetic field, $\mathbf{J} = \nabla \times \mathbf{B}$ is the current density, $\mathbf{v}$ is the plasma velocity and ρ the (uniform) plasma density. The radius of the conducting wall, r_{wall}, is used to normalize lengths, the plasma density is normalized to the uniform density n_0, the magnetic field to the initial value B_0 of the axial magnetic field on axis, velocity to the Alfvén velocity $v_A = B_0/(\mu_0 m_i n_0)^{1/2}$ and time to the Alfvén time $\tau_A = r_{wall}/v_A$. In such units, η corresponds to the inverse Lundquist number, $S^{-1} = \tau_A/\tau_R$ and ν (for a scalar kinematic viscosity) to the inverse magnetic Reynolds number $R^{-1} = \tau_A/\tau_V$, where τ_R and τ_V are the resistive time scale and the viscous time scale, respectively.

The equations are solved in cylindrical approximation with axial periodicity $2\pi R$, implemented on a 100 points staggered radial mesh, with the SpeCyl code, which uses spectral formulation in the angular coordinates [28].

It is worth to note that the approximations used in the model, in particular cylindrical geometry and constant pressure, do not allow to investigate the role of pressure-driven instabilities such as the ballooning modes and the effect of toroidal mode coupling, which could strongly affect the MHD spectrum.

The chosen aspect ratio is that of the RFX-mod device, $R/r_{wall} = 4$; ideal boundary conditions are used to mimic a perfectly conducting rigid wall. As regards to the on-axis values of the adopted dissipation coefficients, they correspond to a Lundquist number $S = 10^5$, which is

considered a good compromise between the upperbound experimental one $S \leq 10^6$ and the need of keeping a reasonable computational time.

The nonlinear behaviour of MHD modes in the ULq configuration, including the effect of finite resistivity, had already been studied in the past by means of 3D MHD simulations as reported in [29, 30]. However, in those works, only $m = 1$ modes were considered, at relatively low Lundquist numbers (up to $S = 10^4$) and the explicit viscous effect was disregarded. A further difference with respect to previous numerical works is that, in those papers, an isolated system was simulated, i.e. no toroidal loop voltage for plasma current sustainment was taken into account [29].

The control parameter in the simulations from the SpeCyl code is the q-value at the wall, which has been driven from $q_{wall} \approx 0$ to $q_{wall} = 1.2$, with a law $q_{wall}(t) = q_{wall}(0) + 1.2t/T_{drive}$, where the duration of the drive is set to $T_{drive} = 6 \times 10^5 \tau_A$. In physical units, taking representative values of magnetic field and density for ULq discharges in RFX-mod, $T_{drive} \approx 180$ ms, which corresponds to a typical discharge duration (see Fig.3). At $t = T_{drive}$ the second part of the simulation starts, with an opposite drive, $q_{wall}(t) = q_{wall}(0) + 1.2(2T_{drive} - t)/T_{drive}$.

Axisymmetric simulations (i.e. with no MHD modes) were at first performed, in order to study the time evolution of the safety factor due to resistive diffusion alone. They were reported in [27] and are omitted here.

When MHD modes are included in the calculation (both 2D, i.e. considering one m/n mode and several of its harmonics and fully 3D simulations have been performed), the time behavior of both q_{core} and q_{edge} turns out to be qualitatively different from that of the 1D unperturbed case. This is particularly evident in the time windows in which some rational surface is crossed by the q-profile and the modes are turned unstable. Such behavior is shown in Figures 7 and 8, where the results of a 3D non-linear simulation are presented.

Fig.7 displays the temporal evolution (indicated with colors) of the safety factor, of the axial and azimuthal magnetic field profiles and of the axial and azimuthal current densities. The shape of the q-profile changes from the typical profile of a paramagnetic pinch configuration to a low-q tokamak profile, during the updrive action on q_{wall} (the opposite trend is found in the downdrive part of the simulation, not shown). In the external region ($r/r_{wall} > 0.85$) a current free condition is imposed (by means of an increasing resistivity profile at the edge), so that all q-profiles follow parabolic curves. It can be observed that the evolution of the radial profiles deep into the plasma region deviates from that expected purely by resistive diffusion, as an effect of MHD modes (in this analysis, the radius $r_{edge} = 0.7 r_{wall}$ is taken as representative for the edge plasma region). Looking in particular at the q profile evolution, it can be observed that the profiles (plotted at uniform time intervals along the upward drive of q_{wall}) tend to accumulate at major resonances in the core (e.g. at the $q = 1/2$ value) due to the effect of MHD activity.

This is investigated more in detail in Fig.8, showing the time evolution of q_{wall}, q_{edge}, q_{core}, along with the amplitude (r.m.s.) of the dominant MHD modes (the toroidal magnetic field component, normalized to the edge poloidal field is chosen, expressed in terms of poloidal and toroidal harmonics). Looking at the upward phase, it is found that q_{edge} follows the external drive but, when it encounters a rational value, it remains fixed to it for a finite amount of time before increasing again up to the next one, where another plateau is found and so on. The simulated evolution of the q-value in the edge plasma region thus resembles the typical staircase behavior observed in the experiment. The plateau phases correspond to rational values with both $m = 1$ and $m > 1$. In particular, shaded grey vertical strips indicate the plateau periods related to the $m = 1$ rational values ($q = 1/4$, $q = 1/3$ and $q = 1/2$). When going from the starting $q_{wall} = 0$ condition to $q_{wall} = 1.2$ (Lq tokamak) the total mode amplitude decreases of about one order of magnitude. Moreover, it is found that in the initial part of the drive many $m = 1$ modes are present simultaneously, together with $m = 0$ modes due to nonlinear coupling. For $t > 1.5 \times 10^5 \tau_A$, the MHD dynamics becomes characterized by a sequence of separate single helicity (2D) modes.

The dynamics of q_{edge} is well time-correlated with that of the MHD modes. In particular, in the evolution of q_{edge} each $m = 1$ plateau phase starts immediately after the disappearance of the $m = 1$ mode with the corresponding helicity. During such plateau phases, $m = 1$ mode amplitude is negligible, whereas a residual finite level of $m > 1$ magnetic activity can be observed. The crossing of each resonance is characterized by almost the same dynamics.

By looking at the down drive phase, a time-reversal symmetry is qualitatively observed, due to the relatively slow (with respect to the resistive diffusion time) down- and up-drive action imposed, with a noticeable staircase-like q_{edge} behavior.

It is worth to note that in the experiment it is difficult to reproduce symmetric upward and downward $q(a)$ drives. In the formation phase of the ULq configuration the raise of the plasma current, at a given applied toroidal magnetic field, and hence the decrease of $q(a)$ from tokamak to ULq values are necessarily faster than that adopted in the theoretical simulation shown in Fig.8. In particular, the crossing of rational q values, and the associated growth of MHD modes, in the plasma current start-up phase is associated with transient increases of plasma resistance. An action as fast as possible (see Fig.8) is thus needed in order to avoid/overcome too strong plasma-wall interaction (PWI) and to reduce the time spent by the discharge in conditions requiring high V_{loop} levels for plasma current sustainment and hence to reduce the consumption of the flux available in the magnetizing winding.

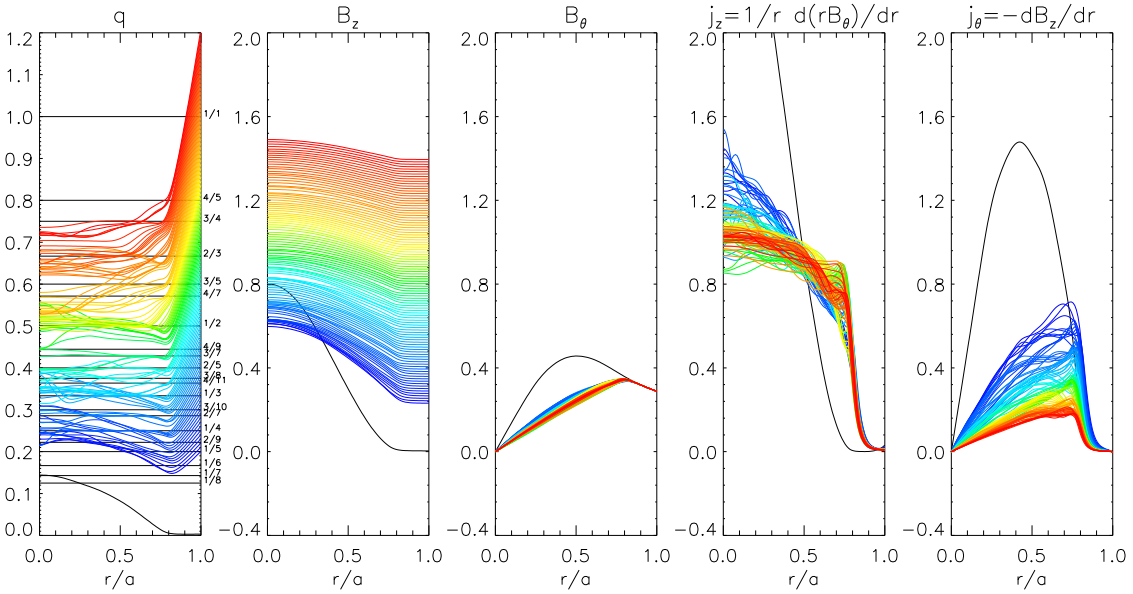

FIG. 7: Time evolution of a 3D simulation with drive of q_{wall}. From the left: radial q-profiles (simulation times indicated with different colors). Axial and azimuthal magnetic field profiles, axial and azimuthal current densities. Black curves refer to the initial profiles used in the simulation. In the left-most figure, black horizontal lines indicate the main rational q values, corresponding to those given on the right y-axis.

Such effect has also been reproduced by 3D simulations (not shown): if the driving action is made fast enough, the MHD modes have not enough time to develop. In particular, when a fast downward q drive is performed, the global single resonant modes have not the time to grow at large amplitude. For instance, when the duration of the drive is reduced to $T_{drive} = 2 \times 10^5 \tau_A$, a clear growth of the 1/2 mode is not observed after the plateau phase of the $q_{res} = 1/2$ resonance.

This is the reason why in Fig.9 only the upward phase of the experimental q value is shown, which corresponds to the slow decay of the plasma current after the flat-top phase, due to a non-optimized discharge control. The same quantities as in Fig.8 are given (apart from the various q values, as only $q(a)$ is directly estimated), with the main difference that, due to the in-vessel diagnostics limitation in mode reconstruction, not the pure $m = 1$ component is shown, but just the odd m component, obtained from the half-difference of signals from probes located on two toroidal arrays in opposite poloidal positions, Fig.9b. For a direct comparison with the theoretical result, time has been normalized to the experimental Alfvén time τ_A, and the estimated amplitude of the various harmonics has been normalized to the edge poloidal equilibrium magnetic field. The color code for the various toroidal and poloidal mode numbers is the same as in Fig.8 (as already mentioned, the maximum detectable poloidal mode number is $m = 3$).

A good qualitative agreement between theoretical and experimental behaviors is found. The discharge exhibits phases of increased magnetic activity, with a quasi-single dominant periodicity, followed by a quiet magnetic phase, corresponding to $q(a)$ plateau windows (highlighted by grey vertical stripes). It is important to note that the agreement is rather good also in a quantitative sense, as the maximum amplitude for each single harmonic is closely comparable to the non-linearly predicted ones (few % of the edge magnetic poloidal field).

As more extensively described in [27], following the results of 2D simulation, the entire MHD process associated with the (updrive) crossing of a resonant q value, q_{res}, can be divided in temporal steps as follows: i) at first, strong kink excitation occurs, with the lowest resonant m/n values, for example 1/2 in the case of $q_{res} = 1/2$. The plasma column is helically distorted at this time and pushed against the wall, where an X-point developes at the rational surface, creating a magnetic island. This is, from an experimental point of view, the phase of maximum PWI (see Fig.6). ii) Kink saturates and double resonance comes in (i.e., the condition in which the $q(r)$ profile has the same rational value in two distinct radial positions), as q_{core} has gone beyond q_{res}. iii) The original m/n is replaced by a m'/n' mode with the same resonant q value but with both double poloidal and toroidal mode numbers (i.e. $m' = 2m$ and $n' = 2n$) in correspondence of a magnetic reconnection event, which doubles the number of magnetic islands and gives rise to the q_{edge} plateau phase. This time instant is indicated in Fig.8c) with a vertical arrow at $t \sim 3.5 \times 10^5 \tau_A$. In this phase, magnetic surfaces lose the typical shift associated with the $m = 1$ kink displacement. Around the resonant value, the q profile is rather flat, and both rational surfaces are at the edge of

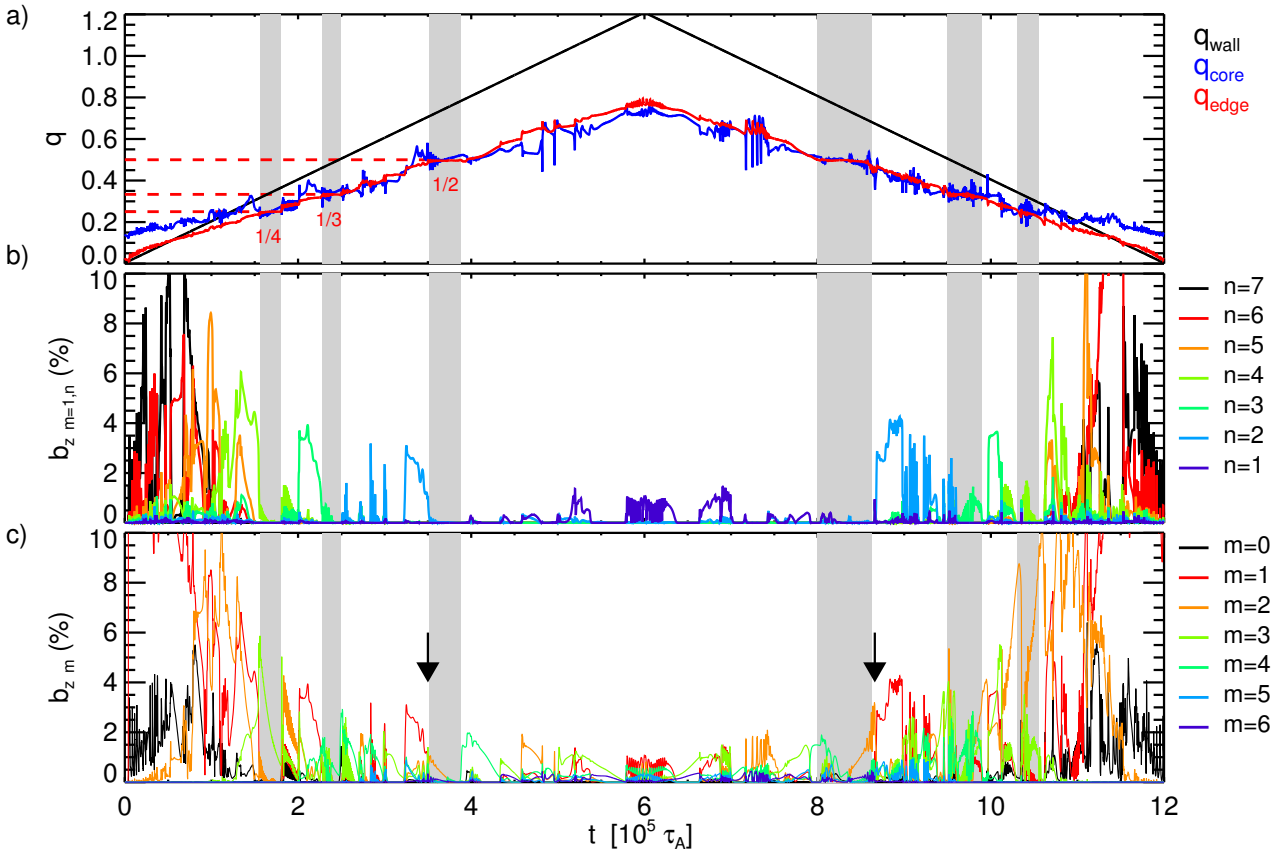

FIG. 8: : 3D simulation for q_{wall} drive. Temporal evolution of (a) the q-value at r_{core}, r_{edge} and r_{wall}; (b) the r.m.s. of the axial magnetic perturbations (different n modes with $m = 1$) normalized to $B_\theta(r_{wall})$ and (c) the r.m.s. of the axial magnetic perturbations (sum over n of different m modes) normalized to $B_\theta(r_{wall})$. ULq regimes are characterized by a sequence of two-dimensional processes excited at the crossing of selected rational q-values. The plateau phases are evidenced by grey vertical bands, the approximate $q(edge)$ value for each stripe is also given. The vertical arrows in panel c) indicate the time instants at which a magnetic reconnection processes occur, in the form of the substitution of a $m = 1(n = 2)$ mode with a $m = 2(n = 4)$ mode and vice versa.

the plasma.

It is worth to note that the presence of the double resonance in the q-profile, which occurs as soon as q_{core} goes beyond q_{res}, is not a sufficient condition for the development of the double resonant mode, which only follows the deflation of the initial kink mode. iv) During the plateau phase, the $m = 2$ mode amplitude decreases, its radial perturbation being localized between the two resonant surfaces, which shrink due to the movement of the internal resonance towards the external one. At a certain point, the $m = 2$ mode disappears and it is replaced by the $m = 4$ mode as a consequence of another magnetic reconnection. The $m = 4$ mode is again a double (tiny) resonant mode, which, following the same path of the preceding $m = 2$ mode, has a decreasing amplitude when two resonances start to approach each other until it also goes out. The plateau phase ends, the MHD process is completed and the configuration is back to an axisymmetric equilibrium.

This kind of dynamics has been also observed in simulation when $q_{res} = 2/5$ is involved in the vacuum region: the $m/n = 2/5$ mode is at first strongly excited as an external mode and becomes double resonant after a reconnection event.

The whole time evolution of the magnetic surfaces for the described process, from $m = 1$ kink destabilization at point i) to the core splitting due to the m=4 mode is shown as contour plot (contour levels of the helical flux function) on an azimuthal cross-section in Fig.10, along with the plasma flow (red arrows).

It is important to emphasize that $m = 1$ double resonant surface modes have never been observed in the numerical simulations. They are indeed linearly unstable, but happen to be suppressed by the nonlinear interaction with $m \geq 2$. This aspect is particularly relevant, as $m = 1$ double resonant surface modes were considered as the most critical issue in past ULq stability analyses [6, 7, 10, 31]. The saturation amplitude of $m \geq 2$ modes, which are rather radially localized, is normally low, so that they are not expected to strongly degrade the macroscopic evolution of the discharge. No information is, however, available about their effect on transport

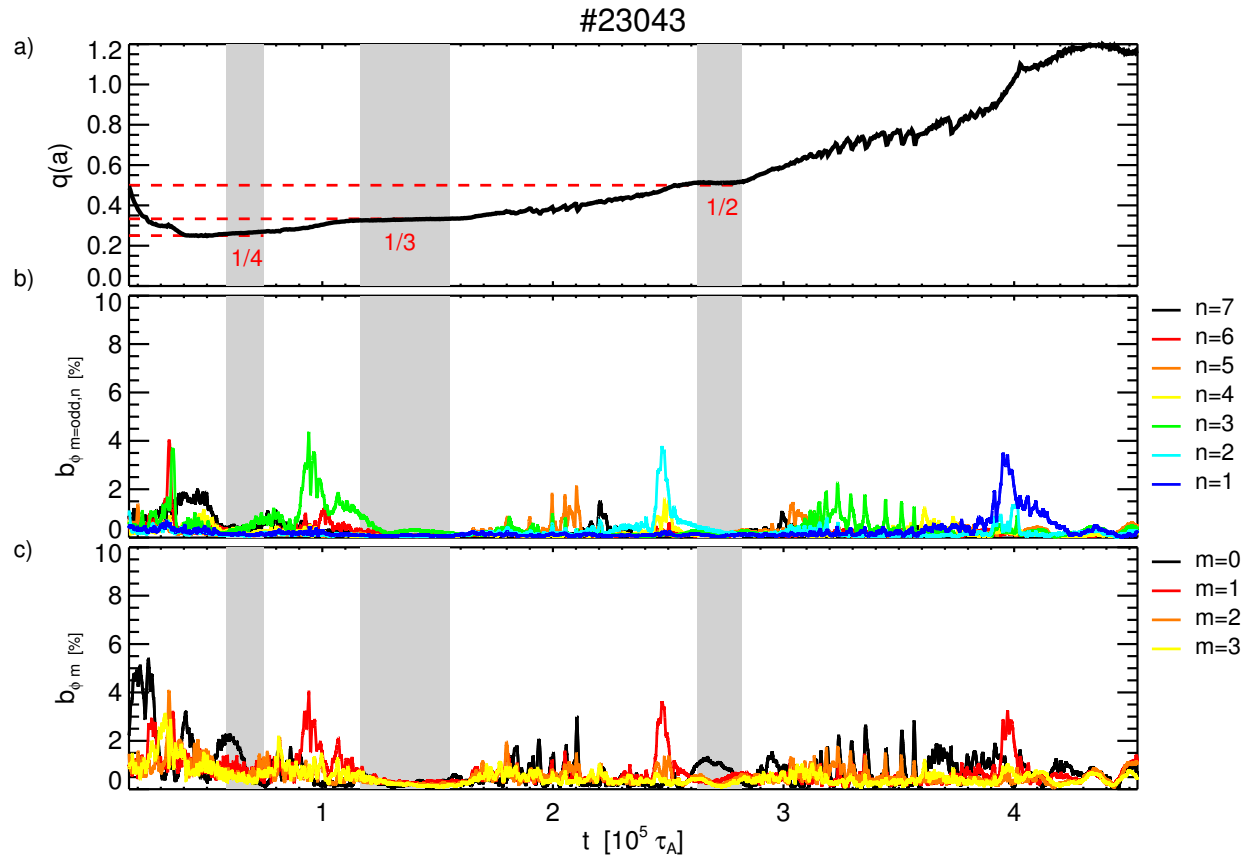

FIG. 9: Temporal evolution of an experimental discharge with a $q(a)$ updrive phase. Time is normalized to the Alfvén time for a comparison with the results shown in Fig.8. Panel a): $q(a)$ evolution; b): amplitude of modes (toroidal component) with odd m and various n numbers (indicated by colors), normalized to $B_\theta(a)$; c): amplitude of modes with various m numbers, indicated by colors, with no distinction in n, normalized to $B_\theta(a)$. The plateau phases are evidenced by grey vertical bands, the approximate $q(a)$ value for each stripe is also given.

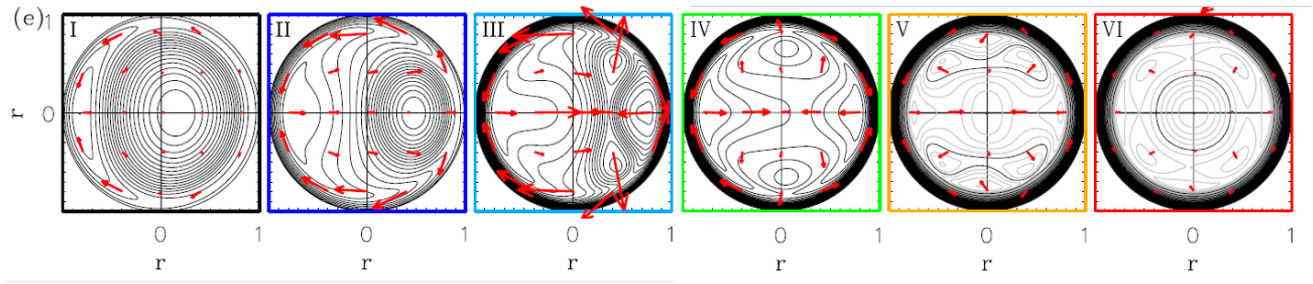

FIG. 10: Contour plots of the Poincaré map of the helical flux function on an azimuthal cross-section at time instants during a magnetic reconnection process. Frame I: strong kink excitation. Frame II: kink saturation and introduction of double resonance. Frames III-IV: core splitting by $m = 2$ double resonant mode and beginning of q_{edge} plateau. Frames V-VI:further splitting of plasma core (by $m = 4$ double resonant mode) and dynamic stabilization. Red arrows indicate the estimated plasma flow.

mechanisms, as these are not included in the model.

When looking at the results of the downdrive 2D simulation, the high-m modes are at first the most unstable ones (for example the $m/n = 4/8$, when $q_{res} = 1/2$ is involved), giving rise to the plateau phase. In concomitance with magnetic reconnection, which induces coalescence (instead of splitting) of magnetic islands, this mode is turned into the $m/n = 2/4$ mode. Later on, the $m/n = 1/2$ kink takes place, the resonant surface disappears and the configuration is axisymmetric again. We can thus conclude that, at least qualitatively, MHD dynamics in the ULq simulation performed is symmetric with respect to time-reversal.

Magnetic reconnection plays a leading role in determining the MHD dynamics in the experiment as well as in the modeling. In Fig.11, the details are

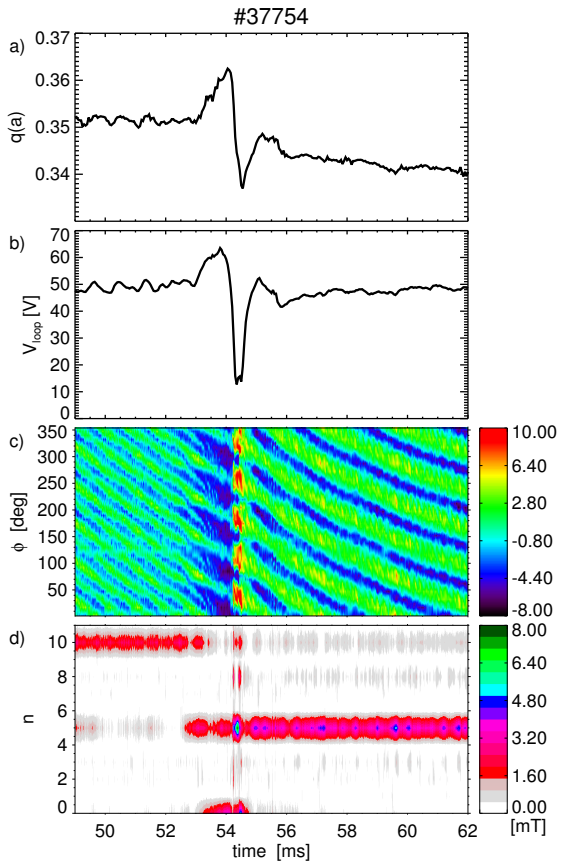

FIG. 11: Time dynamics of single magnetic reconnection event in the experiment: a) edge safety factor, $q(a)$; b) toroidal loop voltage, V_{loop}; c) contour plot of the edge toroidal magnetic field signals along a full toroidal array; d) mode amplitude as a function of the toroidal mode number, n.

proposed of a reconnective dynamics, associated with the coalescence of magnetic islands in a slightly decreasing $q(a)$ discharge. Magnetic reconnection is identified by means of an impulsive variation occurring at t=54 ms of the toroidal loop voltage and $q(a)$ signals in Fig.11b and Fig.11a, sign of a global rearrangement of the current flowing in the plasma. By looking at the color coded contour plots of the in-vessel magnetic signals along a toroidal array, in Fig.11c, and of the mode amplitude as a function of the toroidal mode number, in Fig.11d, it is evident how the reconnection process determines the substitution of a single $m/n = 4/10$, by means of a $m/n = 2/5$ mode, as predicted for the downward drive phase of a $q(a) \approx 0.35$ plasma. However, it important to note that no evidence of the predicted conversion of a $m = 2$ mode to $m = 1$, has been found in the dataase.

It is interesting to note that, from the modeling point of view, no strong differences occur when comparing results on q-profile and topology evolution from 2D (single helicity) and 3D simulations [27]. This suggests that the single helical character is an intrinsic property of ULq plasmas, which is also confirmed by experiments.

The helical flux function deduced during the evolution of a 3D simulation are shown in Fig.12. A strong sensitivity of the magnetic topology on $q(a)$ is clearly visible along with transitions from chaotic to ordered magnetic structures.

These results also indicate that a fine q_{edge} tuning could in principle give access to a sustained configuration with a single saturated kink mode. Such condition, as previously discussed in section II, resembles that encountered in high current RFP plasmas, both in the experiment and in MHD modeling [21]. With the purpose of exploring the feasibility of stable helical ULq equilibrium, 3D simulations with stationary conditions have been produced. In particular, q_{wall} sustainment was forced at values slightly above few relevant resonances. It has been found that, depending on the final q_{wall} value (0.5, 0.67 and 0.76 were considered) either stable helical state with a large global single saturated mode (1/2 in the q_{wall}=0.5 case) or a quasi-axisymmetric state with a tiny localized ($m = 4$) double resonant mode (see Figs. 8 and 9 in [27]) appear. The sustainment, though verified in principle, could be difficult to perform in the experiment, due to the exhibited high sensitivity to $q(a)$. Nonetheless, examples of both behaviors have been found in the RFX-mod database; two of them are shown in Fig. 13.

In particular, in the first example (left column of Fig.13) a case with a very tiny MHD (almost quiet) activity is presented. No clear magnetic structure is visible, and $q(a)$ remains almost stable for a 30 ms time window ($\approx 10^5 \tau_A$), in agreement with theoretical expectation (see Fig. 8 in [27]). In the second example, in the right column of the same figure, $q(a)$ exhibits a 30 ms plateau phase, associated with a long lasting saturated 2/5 mode. The mode is observed to rotate with a quasi-constant frequency, an aspect which will be discussed in the dedicated section.

Along with such stable equilibria, strongly fluctuating discharges have been successfully sustained. One of these plasmas, with two phases at $q(a) \approx 0.365$ and $q(a) \approx 0.39$, respectively, is presented in Fig.14. Both phases are characterized by an intense sawtooth-like behavior, due to the action of two distinct modes. At first, $45 < t < 65$ ms a bursty 3/8 mode is dominant, while in the second phase, $75 < t < 110$ ms corresponding to $q(a) \approx 0.39$, the 2/5 has the largest (fluctuating) amplitude. The activity of such modes and the correlation with the fluctuation of $q(a)$, closely resembles what described by 3D simulation (see Fig. 10 in [27]), where the modes responsible for the q profile oscillation are predicted to be double resonant high m modes. In Fig.14, along with $q(a)$ and mode amplitude, the time traces are given of the plasma current, I_p (panel b) and of the edge and radially averaged toroidal magnetic fields, $B_\phi(a)$ and $< B_\phi >$, respectively, (in panel c). In panel d, the toroidal loop

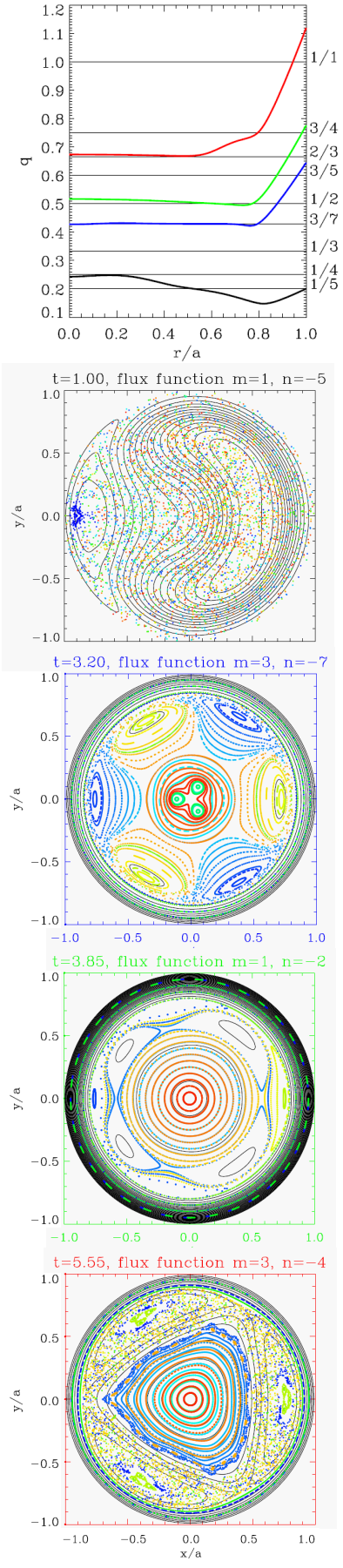

FIG. 12: From the left: Radial q profile at few chosen time instants during the evolution of the 3D simulation shown in Fig.8; contour plots of the Poincaré map of the helical flux function on an azimuthal cross-section for the same time instants (indicated with colors). The dominant m/n mode for each frame is indicated.

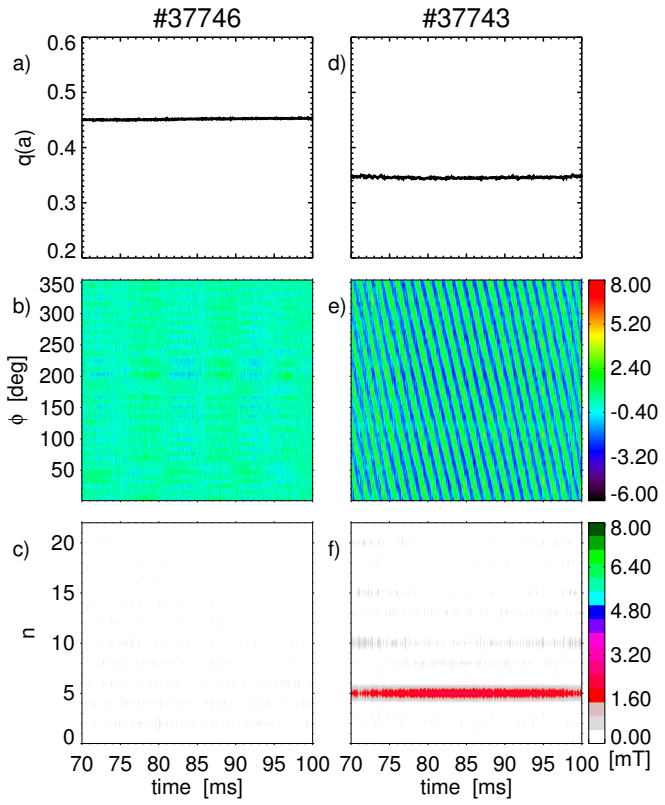

FIG. 13: Time behavior of two discharges with a long lasting quasi-stationary phase. Left column shows a discharge with a very tiny MHD activity; right column shows a conditions with a saturated helical (2/5 mode; a) and d): edge safety factor, $q(a)$; b) and e): contour plot of the edge toroidal magnetic field signals along a full toroidal array; c) and f) mode amplitude as a function of the toroidal mode number, n. Color scale is the same for left and right columns.

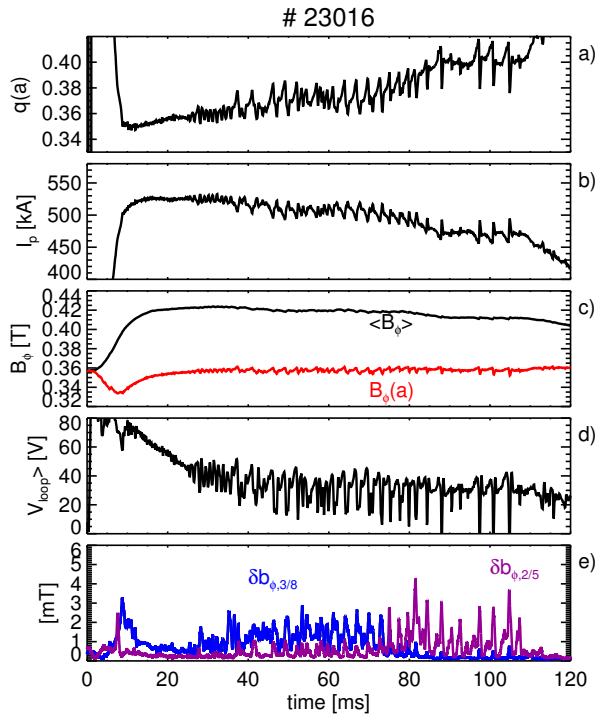

FIG. 14: Example of a sustained discharge with oscillating edge safety factor $q(a)$ in panel a). Other panels: time traces of: b) plasma current I_p; c) edge (red curve) and average toroidal magnetic fields (black curve), $B_\theta(a)$ and $< B_\phi >$, respectively; d) toroidal loop voltage, V_{loop}; e) amplitude of the magnetic perturbation at the edge (toroidal component) for the 3/8 (blue curve) and the 2/5 (violet) modes.

voltage is shown. All quantities exhibit fluctuations, with a different relative amplitude. In particular, for the case shown, $\delta q(a)/q(a) \approx 9\%$, $\delta I_p/I_p \approx 7\%$, $\delta B_\phi(a)/B_\phi(a) \approx 2\%$, $\delta < B_\phi > / < B_\phi > \approx 0.4\%$, which indicates that most of $q(a)$ fluctuations is due to perturbation of the toroidal plasma current. This situation is somehow different from what observed in RFP plasmas, where reconnection processes globally rearranging the magnetic topology, induce large impulsive generation of toroidal flux (the so-called discrete dynamo action), with a lower effect on the toroidal plasma current [32].

C. External kinks in the presence of a resistive shell: the role of the magnetic feedback control

As mentioned, in RFX-mod the plasma is surrounded by a thin copper shell (with an effective penetration time for a vertical field equal to $\tau_b \approx 70$ ms) and is covered, as described in section II, by 48×4 (along the toroidal and the poloidal direction, respectively) saddle coils with independent power supplies; radial field sensor loops of the same size are located inside the shell. Real time currents in the saddle coils are driven by a digital central control system, which, by means of software-implemented feedback algorithms, processes sensor measurements.

The simplest control scheme, dubbed "virtual shell" (VS) [20], is adopted when the flux through each sensor loop is controlled by the corresponding active coil. Such scheme closely approaches the intelligent shell as proposed in [33]. In particular, in the VS scheme, the control system determines the currents flowing into the saddle coils in order to keep the measurement of the corresponding sensor coils as close to zero as possible.

In RFP operations, the VS scheme proved to be successful in reducing the edge radial field on time scales longer than the shell penetration time [34], thus allowing to sustain RFP discharges much longer than those with passive shell action only. Such scheme was proven able to completely stabilize the resistive wall modes (which in RFX-mod have $m = 1, n < 6$, respectively [20, 35]. The VS scheme was, however, less effective on the edge value of the perturbation associated to tearing modes (TMs) due to the aliasing, which affects the measured magnetic field harmonics. The aliasing is due to the high poloidal and toroidal mode number sidebands produced by the discrete coils grid. In order to correct such effect, under the reasonable assumption

that the pollution of the Discrete Fourier Transform (DFT) harmonics is only due to the saddle coils sidebands and not to MHD modes, a cleaning algorithm named Clean Mode Control, CMC, scheme had been developed [36] and widely used with good success in the highest plasma current campaigns of RFX-mod. In order to properly apply the CMC scheme to RFP (and tokamak) plasmas, extensive preliminary work was dedicated to the optimization of control algorithms and parameters to be implemented in real time. Due to the limited experimental time, such optimization was not obtainable for the ULq campaigns, so that in most of the discharges the VS feedback scheme was adopted (only in a third campaign, operating with Deuterium, the CMC scheme was used, but with the optimized control papameters for RFP operations, which have been $a-posteriori$ demonstrated to be unsuited for ULq ones). On few specific discharges, the feedback action has been disabled on purpose.

When no feedback control is applied, a slowly growing externally resonant m/n=1/1 mode has been observed to emerge within the magnetic spectrum as in the case shown in Fig.15 with red curves. In the e) panel of the figure, the amplitude of this mode is found to almost exponentially increase with a growth time around 30 ms ($\gamma\tau_w \approx 2$) in the flat-top phase of the discharge with $q(a) \approx 0.5$. The phase of the mode is almost constant in time, which means that $\omega\tau_w \ll 1$, as also occurs for the resistive wall modes (RWM) in the RFP. This observation confirms previous observations in HBTX-1C [12] about the growth of a 1/1 mode, in the presence of a resistive shell. In that study, the slow growth of the mode continued until termination of the discharge. The onset of the 1/1 mode was retarded, for a given $q(a)$ value, by increasing the toroidal applied field. The growth of the 1/1 mode is also accompained by an increase of the light impurity (Carbon and Oxygen) influxes (panel g and h), while no effect on the working gas (Hydrogen in this case in panel f) influx is visible. This result is an indication of the localized interaction of the plasma with a low Hydrogen recycling graphite first wall due to the 1/1 displacement. In Fig.15, the time behavior of a discharge with applied VS feedback scheme is also shown (blue curve). The control system is effective in suppressing the 1/1 mode, which remains at an almost negligible amplitude for the whole flat-top phase, corresponding to a strong reduction of the impurity content. An abrupt change of growth rate of the 1/1 mode is observed in both discharges during the ramp-down phase of the plasma current. In particular, at the time in which $q(a)$ crosses a value close to 0.8 (indicated by red and blue dotted vertical lines in the figure), the mode exhibits a period of strong increase with a characteristic growth time of about 5 ms. This phase is followed by an abrupt decrease of the plasma current (and a corresponding increase of $q(a)$). When $q(a) \gtrsim 1$ spontaneous stabilization of the 1/1 occurs, which can be interpreted as a clear example of the classic Kruskal-Shafranov criterion [48].

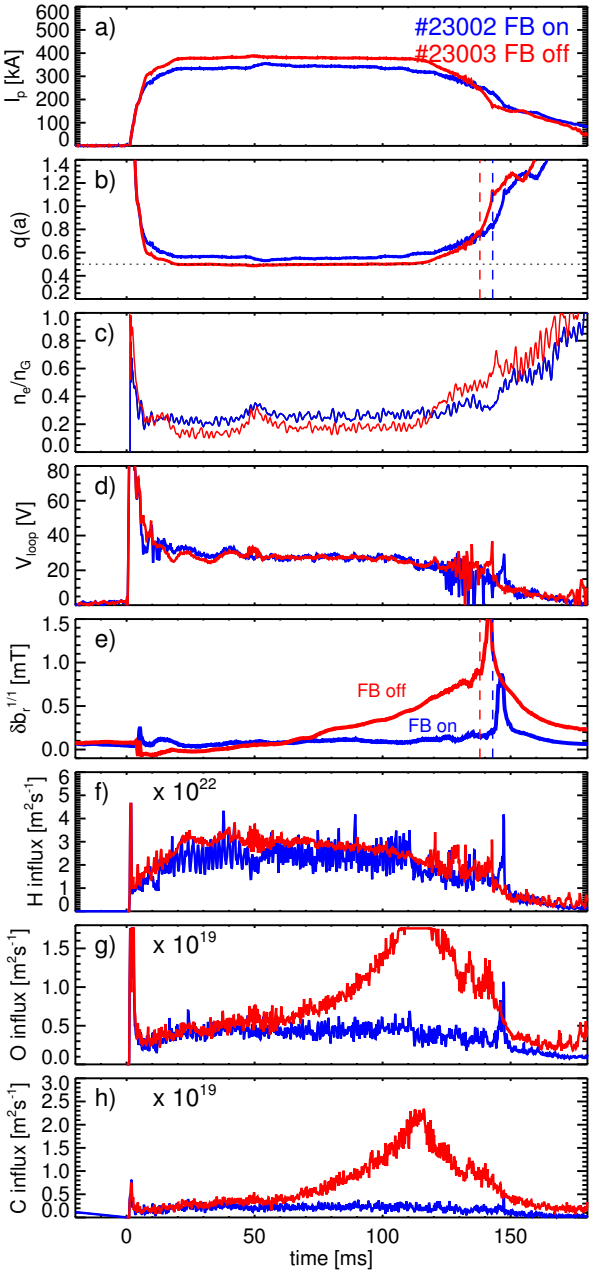

FIG. 15: Time hystory of two shots the first (blue curves) with FB control of the 1/1 external kink mode, the second (red curves) without FB. a) Plasma current, I_p; b) edge safety factor, $q(a)$; c) normalized (central) electron density, n_e/n_G; d) toroidal loop voltage, V_{loop}; e) amplitude of the 1/1 mode (radial magentic field component); f), g) and h) H, O, C particle influxes, respectively, as measured from a central chord.

The dependence of the 1/1 growth rate, $\gamma^{1/1}$ on $q(a)$ with no active feedback control is shown in Fig.16 on a statistical basis. Each point is an average over different shots (most of the $q(a)$ range is covered by slowly decaying plasma current conditions), the growth rate being determined from an exponential fit over 5 ms

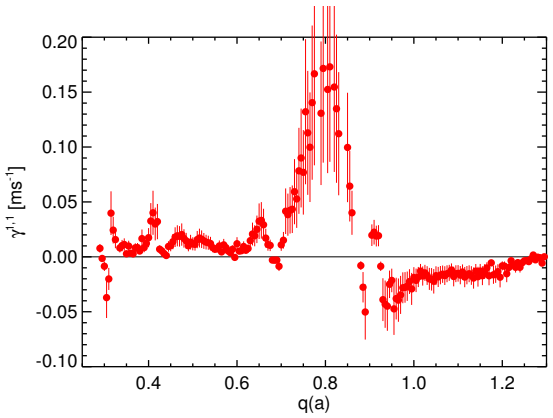

FIG. 16: Growth rate, $\gamma^{1/1}$ of the 1/1 mode as a function of $q(a)$ in discharges with no active feedback control. Each point is an average over different shots (most of the $q(a)$ range is covered by slowly decaying plasma current conditions), the growth rate being determined from an exponential fit over 5 ms time windows.

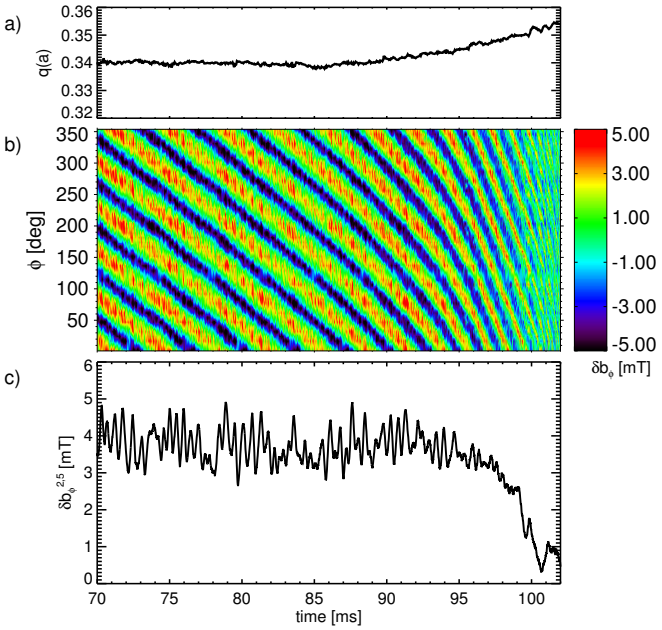

FIG. 17: Time evolution of an ULq discharge with spontaneous toroidal mode rotation. a) Edge safety factor, $q(a)$; b) contour plot of the edge toroidal magnetic field along a toroidal array; c) amplitude of the dominant 2/5 mode, $\delta b_\phi^{2/5}$. Mode acceleration occurs starting at 90 ms, correlated to mode amplitude decrease.

time windows. $\gamma^{1/1}$ exhibits a maximum value 0.2 ms^{-1} for $q(a)$ around 0.8, Local maxima at $q(a) \approx 0.4$ and $q(a) \approx 0.7$, while a tight $q(a)$ windows of 1/1 marginal stability ($\gamma \sim 0$) seems to occur for $q(a) \approx 0.66$. Plasmas with $q(a) > 0.95$ are found to be stable with respect to the 1/1 mode, in agrement with the Kruskal-Shafranov criterion.

D. Mode rotation

In a large part of the ULq database, MHD modes exhibit a spontaneous rotation in the toroidal direction at frequencies spanning from tens of Hz up to few kHz, depending on the experimental condition. As can be seen in Fig.13 (right column), such rotation can be regular, i.e. mode velocity remains constant for a time window comparable to the flat-top duration. In some cases, the mode exhibits acceleration and deceleration phases, which occur spontaneously as a consequence of the mode dynamics; an example is given in Fig.17.

A 2/5 mode dominates the MHD spectrum, as clearly visible in panel (b), where a contour of the ISIS toroidal magnetic signals at the edge as a function of time and toroidal angle is presented (five maxima are visible). The mode rotates at a constant frequency (around 300 Hz) until $t \approx 90$ ms, when it starts accelerating. The frequency more than triples in 5 ms. Such acceleration is associated with a spontaneous decrease of mode amplitude (see panel c), likely to be induced by an equilibrium profile evolution. $q(a)$ is, indeed, slightly increasing from $t \approx$85 ms (panel a).

A similar dynamics is also observed in largely fluctuating discharges, in which a sequence of mode acceleration and deceleration related to the $q(a)$ dynamics is found. In particular, as shown in Fig.18, during the acceleration phase of the dominant 3/8 mode lasting less than 300 μs in the upward $q(a)$ drive, the frequency changes from less than 1 kHz to more than 10 kHz. In the decrease phase of $q(a)$ extremely fast mode deceleration occurs. For the sake of clarity, the phase of the mode $\Phi^{3/8}$ is also shown in panel c), along with mode amplitude $\delta b_\phi^{3/8}$ and mode frequency (estimated from $\frac{d\Phi^{3/8}}{dt}$). Mode amplitude and $q(a)$ dynamics are almost $\pi/2$ phase shifted as it can be observed in the hodogram (i.e. $\delta b_\phi^{3/8}$ *vs* $q(a)$) in Fig.19. It is interesting to note that the transition from the slow to the fast rotation branch occurs when mode amplitude falls below 2 mT (red dots in Fig.20).

No hysteresis phenomenon is observed during the inverse transition, when the mode starts again to increase (blue dots) above almost the same threshold. This is a relevant result in particular when compared to what occurs in RFP discharges in RFX-mod. It is well known that tearing modes co-rotation with the plasma mitigates their amplitudes, the radial field being screened at the location of the innermost conductive wall (often the vacuum vessel). It is worth here noting that intrinsic plasma rotation has been analyzed in RFP plasmas in the MST device, where magnetic-fluctuation induced kinetic stress is observed to act as a force driving plasma flow [41].

This natural mode rotation easily ceases, as the image currents induced onto the wall develop a braking

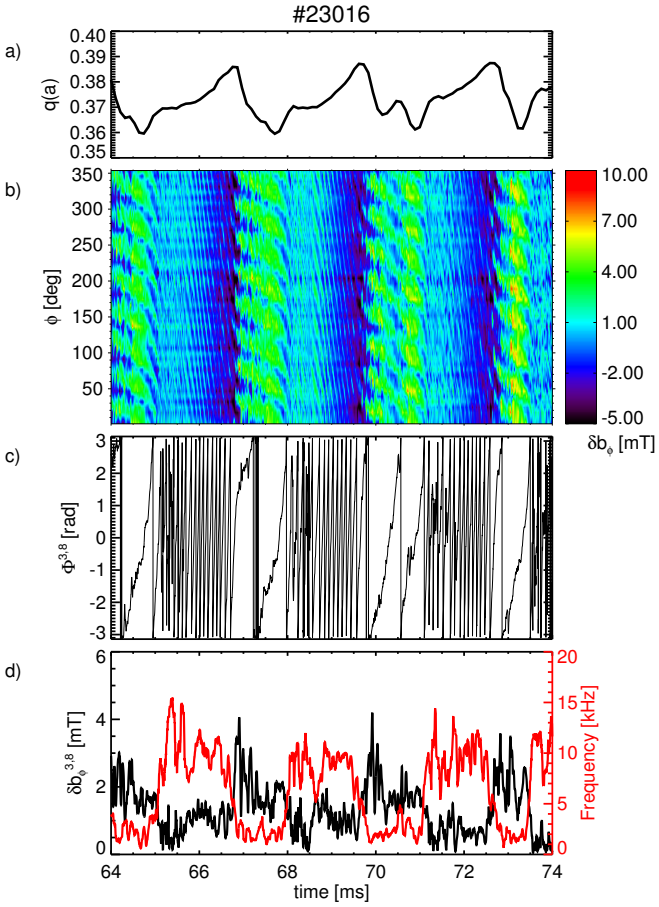

FIG. 18: Time traces of a fluctuating discharge exhibiting a sequence of acceleration/deceleration phases. a): edge safety factor q(a); b) contour plot of the toroidal magnetic field fluctuations along the toroidal angle; c) phase of the dominant 3/8 mode, $\Phi^{3/8}$; d) amplitude (black curve) and frequency (red curve) of the 3/8 mode.

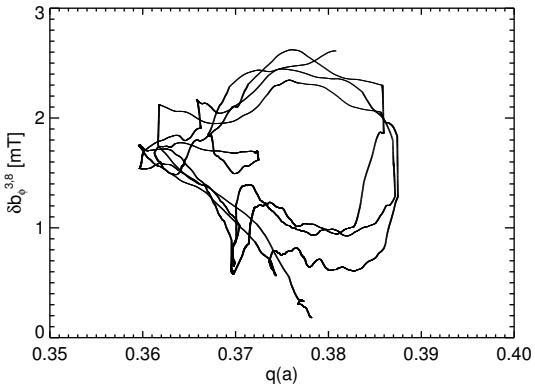

FIG. 19: Hodogram of the amplitude of the 3/8 dominant mode (toroidal component) as a function of $q(a)$ for few cycles of the $q(a)$ oscillations for the shot #23016.

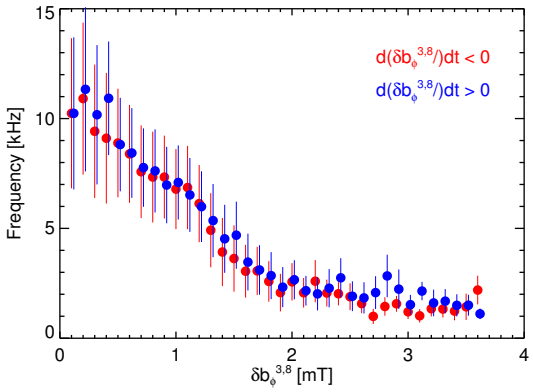

FIG. 20: 3/8 mode frequency as a function of its amplitude (toroidal component) for few cycles of the $q(a)$ oscillations for the shot #23016.

electromagnetic torque, which stops tearing modes in the laboratory frame (wall-locking) as soon as their amplitude at the resonant surface exceeds a threshold [37, 38]. When this threshold is overcome, radial magnetic field penetrates the wall at a rate determined by the wall time-constant [39]. The phenomenon is particularly dangerous because of the hysteresis which characterizes it: it is theoretically predicted that tearing amplitude at the resonant surface must be significantly reduced below the wall-locking threshold to recover the spontaneous rotation [37]. This hysteresis can thus make wall-locking to become irreversible, potentially disruptive, process. Wall-locking is common to both tokamak and reversed field pinch (RFP) devices.

Indeed, as presented in [42], RFP discharges in RFX-mod are characterized by the presence of many non-linearly interacting internally resonant modes with comparable amplitude. For plasma current above the threshold $I_{p,th} \approx 100$ kA, the RFP internal modes are normally locked to the wall and the non-linear mode coupling induces a phase-locking and a toroidally localized bulging of the plasma column (the so-called "slinky"-mode)[49]. Enhanced local plasma-wall interaction can thus take place. In order to avoid extremely high power load to the first wall, the feedback system is routinely exploited in RFX-mod to force a slow (of the order of few tens of Hz) differential toroidal mode rotation. Thanks to the exploitation of the feedback system it was possible to recover the fast rotation with no hysteresis when reducing mode amplitude.

In the ULq case, shown in Fig. 20, the mode has a $m = 3$ poloidal mode number, which is not within the spectrum available for feedback control (as mentioned, the maximum controllable m is 2). The reversible transition from fast to slow rotation branch in the ULq thus appears as a spontaneous phenomenon, with no effect from external action. Even more relevant, no dangerous wall-locking is normally observed.

In order to clarify the differences, between the two

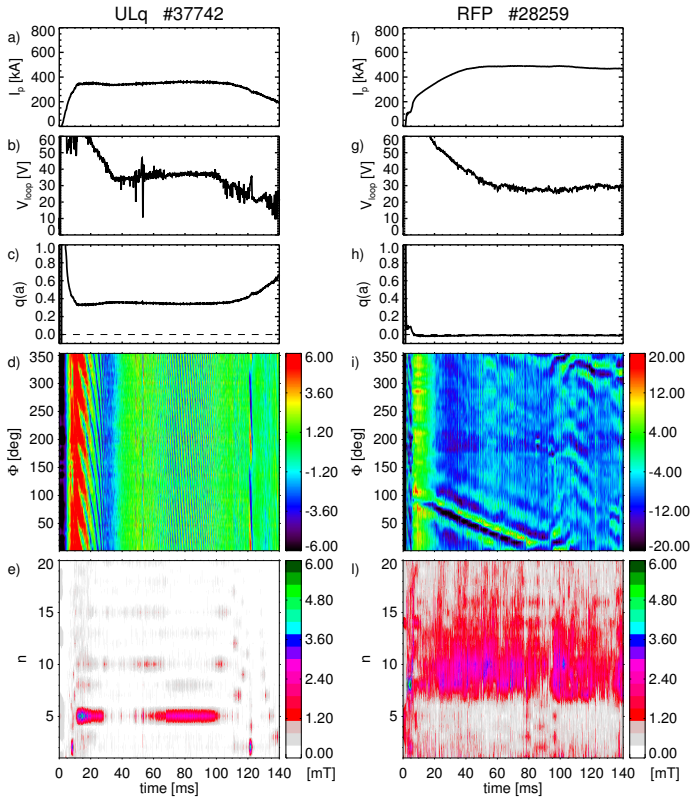

FIG. 21: Time history of ULq (left column) and RFP (right column) discharges at comparable plasma current level. a) and f) plasma current, I_p; b) and g) toroidal loop voltage, V_{loop}; c) and h) edge safety factor, $q(a)$; d) and i) contour plot of the toroidal magnetic field fluctuations along a toroidal array; e) and l) mode amplitude as a function of the toroidal mode number, n. In panel i) a localized structure (slinky mode) is observed to form at t =15 ms around $\phi = 70°$ and then to slowly move (externally controlled induced rotation) along the toroidal angle.

configurations, in Fig.21 a direct comparison between ULq and a RFP discharges, with similar plasma current levels (350 kA and 400 kA, respectively) is presented. In the left column, the time evolution of a $q(a) = 0.4$ ULq plasma is shown, with a saturated $n = 5$ dominant mode in the fast rotation branch for most of the flat-top phase. In the right column, the typical features of a relatively low-current RFP plasma in RFX-mod can be recognized. In the contour plot of the toroidal magnetic field signals, in Fig.21i, a localized structure forms in the start-up phase of the discharge, at a toroidal angle close to $\phi \approx 70°$. This perturbation, associated with the mentioned slinky mode, is kept at slow rotation (few Hz) by the action of the external feedback system. The broadband magnetic spectrum in Fig.21l is populated by instabilities with mode numbers $n \geq 7$, being $m/n = 1/7$ the most internally resonant mode for the chosen equilibrium. Mode rotation, which is not taken into account by the MHD simulations, makes the ideal boundary condition a better approximation in the ULq than in the RFP, at least for what concerns the discharges produced in the RFX-mod device. It is worth to note that the spontaneous transition from the control-induced slow mode rotation to the spontaneous high frequency one (at few kHz, mainly determined by the electron diamagnetic drift [42]) is found in RFX-mod in RFP plasmas only for plasma current below the mentioned 100 kA current threshold, which corresponds to a mode amplitude threshold of less than 0.5 mT. Such value is much lower than the one measured in ULq plasmas (see Figs.17 and 18), which almost ubiquitously exhibit a single dominant fast rotating mode, even at amplitude above 4 mT.

IV. DISCUSSION

The safety factor profile in the ULq configuration normally exhibits a pitch minimum at the edge (removed in the RFP equilibrium), which has been theoretically predicted in the literature to lead to both pressure driven and current driven instabilities, also in the form of double resonant surface modes.

In the experimental campaigns of RFX-mod considered here, ULq plasmas have been produced in a wide range of conditions, mainly in terms of plasma current and edge safety factor. The predicted relevant role of the edge safety factor $q(a)$ in determining plasma dynamics is observed in the experiments; in particular, slight changes of the equilibrium produce either largely fluctuating or quiet discharges.

The spectral properties of the observed MHD activity, deduced from highly space-time resolved in-vessel magnetic probes are in good qualitative and quantitative agreement with the results of dedicated non-linear 3D visco-resistive MHD simulations. In particular, the predicted tendency of ULq spectra to be dominated by a single resonant mode (either a kink or a double resonant internal mode) is confirmed by the experiments. Quiet plasma phases, with almost non-detectable magnetic fluctuation, lasting up to tens of ms are observed at discrete $q(a)$ values. The loop voltage necessary to sustain the discharge in the flat-top phase is comparable to or slightly larger than that in the RFP in the same plasma current condition.

It is important to observe that $m = 1$ double resonant surface modes, demonstrated by theoretical analysis in the past to be linearly unstable, turn out to be suppressed in 3D nonlinear simulations by the (nonlinear) interaction with $m \geq 2$. This aspect is of great relevance, as $m = 1$ double resonant surface modes were considered an extremely critical issue for the confinement performance of the ULq configuration. Experiments confirmed that no critically unstable $m = 1$ modes are generally present within the MHD spectrum.

Moreover, magnetic reconnection plays a relevant role in determining the dynamics of the magnetic topology. It can induce coalescence or splitting of

magnetic islands, a dynamic process normally followed by relatively long lasting (of the order of 10 ms) plateau phases of the plasma current, with almost quiescent MHD activity. Differently from what predicted by modeling, the reconnection phenomena occuring in the RFX-mod plasma, experimentally recognized as rapid reconfiguration of the magnetic topology indicated by large spikes of the loop voltage signal, are associated with the activity of modes with relatively high poloidal mode numbers $m \geq 2$.

The complex active feedback magnetic control system of RFX-mod (not yet optimized for such plasmas) has been exploited in order to suppress the externally resonant $m/n = 1/1$ mode, whose growth rate has been characterized in wide range of $q(a)$ plasmas. The succesfull control of the 1/1 mode is a key ingredient in order to avoid fast discharge termination in the ULq.

Differently from what ecnountered in RFP plasmas at comparable current levels, MHD modes exhibit toroidal rotation at a frequency in the kHz range, depending on mode amplitude. The spontaneous transition from a fast to slow rotation branch and vice versa occurr, with no wall locking and no hysteresis even in the absence of the action of external active MHD control.

The analysis of the MHD activity in the ULq will be in the near future complemented by the characterization of the confinement and transport properties, which will be the topic of a dedicated paper.

Of particular relevance, in our opinion, will be the analysis of the observed possibility of overcoming the Greenwald limt with no disruption or radiative collapse [13]. Moreover, previous studies indicate that the ion temperature can become significantly larger than the electron temperature in ULq plasmas, which can be efficiently sustained by Ohmic heating only [11].

V. CONCLUSION

Thanks to its flexibility and unique control capability due to the advanced MHD modes feedback system made of 192 independently driven saddle coils, the toroidal RFX-mod device for magnetic confinement of fusion plasmas can be operated to investigate a wide range of experimental conditions. In order to highlight similarities and/or physics peculiarities between various magnetic configurations, Reversed-Field Pinch (RFP), Tokamak and the full range of magnetic configurations in between the two, the so-called ultra-low q (ULq), which corresponds to edge safety factor values positive and below 1, have been produced.

The ULq experiments here considered have been inspired and complemented by an intense theoretical activity, based on 3D non-linear MHD modeling. The results presented mainly concern the rich MHD behaviour and modes rotation, which are compared to those obtained in RFP plasmas produced in the same experimental device.

The natural tendency of ULq plasmas towards preferred $q(a)$ value has been observed both in the experiment and in the simulation. Slight changes of $q(a)$ can induce a transition from almost fluctuation free to largely sawtoothing plasmas. The magnetic spectrum is typically dominated by one single helicity, which is associated to modes exhibiting spontaneous rotation. No wall-locking phenomenon has been observed even without MHD feedback control. As predicted by simulations, magnetic reconnection in time-varying $q(a)$ phases produces abrupt changes in the magnetic topology and in the fluctuation spectrum.

The Authors believe that, despite the fact that the ULq configuration lost interest as a viable fusion device back in 80's, it still shows some attractive features, which deserve to be studied. Only part of these features have been thoroughly explored in this paper and include a relatively simple MHD dynamics basically determined by the external control of the $q(a)$ value. The interesting behavior of the ion temperature dynamics in Ohmically heated plasmas, as reported in the exisiting literature is worth of further experimentation. In particular, the possibility that during reconnection events part of the magnetic energy is converted into ion heating and acceleration, with a consequent enhancement of the neutron flux from fusion reactions, as observed in RFP plasmas, will be the subject of future investigations along with the analysis of the confinement properties of the wide and varied range of ULq configurations.

[1] S. Glasstone and R.H. Lovberg, Controlled Thermonuclear Reactions, Ed. by D. Van Nostrand Company, Inc., Princeton, New Jersey, (1960)
[2] J. Sheffield, Rev. Mod. Phys. 66, 1015 (1994)
[3] R.D. Hazeltine and J.D. Meiss 1992 Plasma Confinement (Reading, MA: Addison Wesley)
[4] D.E. Evans, Pulsed High Beta Plasmas, Pergamon Press, Oxford (1976)
[5] P.C. Thoneman, Nature (London) 181, 217 (1958)
[6] D.C. Robinson , Plasma Phys. 13, 439 (1971)
[7] Y. Murakami et al, Nucl. Fusion 28, 449 (1988)
[8] Z. Yoshida, S. Ishida, K. Hattori, Y. Murakami, J. Morikawa, H. Nihei, and N. Inoue, J. Phys. Soc. Jpn 55, 450 (1986)
[9] Z. Yoshida, K.Kusano, and N. Inoue, The Physics of Fluids 30, 2465 (1987)
[10] Y. Kamada et al, Nucl. Fusion 29, 713 (1989)
[11] T. Fujita et al., Nucl. Fusion 31, 1 (1991)
[12] H.Y.W. Tsui et al, Nucl. Fusion 30, 59 (1990)
[13] M. Zuin, S. Dal Bello, L. Marrelli, M. Puiatti, P. Agostinetti, M. Agostini, V. Antoni, F. Auriemma, M. Barbisan, T. Barbui, et al., Nuclear Fusion 57, 102012

(2017)
[14] P.L. Taylor et al., Nucl. Fusion 29(1), 92-95 (1989)
[15] M. Watanabe et al., Journal of Nuclear Materials 220-222, 641-645 (1995)
[16] J.S. Sarff, S.A. Hokin, H. Ji, S.C. Prager, C.R. Sovinec, Phys. Rev. Lett. 72, 36703673 (1994)
[17] B.E. Chapman et al., Phys. Plasmas 9, 20612068 (2002)
[18] Z. Yoshida, T. Uchida, and N. Inoue, Phys. Fluids 27, 1785 (1984)
[19] S. Cappello and D.F. Escande, Phys. Rev. Lett. 85, 3838 (2000)
[20] R. Paccagnella et al., Phys. Rev. Lett. 97, 075001 (2006)
[21] R. Lorenzini et al., Nature Phys. 5 (8), 570 (2009)
[22] P. Piovesan et al., Nucl. Fusion 49 (8), 085036 (2009)
[23] P. Piovesan et al., Phys. of Plasmas 20 (5), 056112 (2013)
[24] G. Serianni G et al, Rev. Sci. Instrum. 75, 4338 (2004)
[25] V. Antoni and S. Ortolani, The Physics of Fluids 30, 1489 (1987)
[26] D. Bonfiglio et al., Phys. Rev. Lett. 111, 085002 (2013)
[27] D. Bonfiglio et al., Nucl. Fusion 48 (11), 115010 (2008)
[28] S. Cappello and D. Biskamp, Nucl. Fusion 36, 571 (1996)
[29] K. Kusano et al, Nucl. Fusion 28, 89 (1988)
[30] K. Suzuki et al, Nucl. Fusion 31, 179 (1991)
[31] K. Itami et al, Nucl. Fusion 28, 1535 (1988)
[32] M. Zuin et al.,Plasma Phys. Control. Fusion 51, 035012 (2009)
[33] C.M. Bishop, Plasma Phys. Control. Fusion 31, 1179 (1989)
[34] S. Ortolani et al, Plasma Phys. Control. Fusion 48, B37181 (2006)
[35] T. Bolzonella et al, Fusion Eng. Des. 82, 1064 (2007)
[36] P. Zanca et al., Nucl. Fusion 47, 1425-1436 (2007)
[37] R. Fitzpatrick Nucl. Fusion 33, 1049 (1993)
[38] S.C. Guo and M.S. Chu Phys. Plasmas 11, 4050 (2004)
[39] C.G. Gimblett Nucl. Fusion 26, 617 (1986)
[40] G. Spizzo, G. Pucella, O. Tudisco, M. Zuin, M. Agostini, E. Alessi, F. Auriemma, W. Bin, P. Buratti, L. Carraro, et al., Nuclear Fusion 55, 043007 (2015)
[41] W.X Ding et al., Phys. Rev. Lett. 110, 065008 (2013)
[42] P. Innocente, P. Zanca, M. Zuin, T. Bolzonella and B. Zaniol, Nucl. Fusion 54, 122001 (2014)
[43] Z. Yoshida et al., Nucl. Fusion, 31, 8 1532-1535 (1991)
[44] Z. Yoshida, Physics of Fluids B: Plasma Physics 4, 1534 (1992)
[45] Z. Yoshida et al.J. Plasma Phys. 59, 103 (1998)
[46] L.Marrelli et al., Nucl. Fusion 61, 023001 (2021)
[47] M. Zuin, Magnetic Confinement FusionExperimental Physics: Reversed Field Pinches, Reference Module in Earth Systems and Environmental Sciences, Elsevier, 2021,
[48] H. Zohm, Magnetohydrodynamic Stability of Tokamaks, Ed.WileyVCH Verlag GmbH & Co. KGaA (2014)
[49] K. Kusano and T. Tamano and T. Sato, Nucl. Fusion 31, 1923 (1991)